Investigating the tumour-intrinsic role of programmed death-ligand 1 in 2D and 3D cell culture models of human breast cancer

HUDSON, Katie, CROSS, Neil <http://orcid.org/0000-0003-2055-5815>, JORDAN-MAHY, Nicola and LEYLAND, Rebecca

Investigating the Tumour-Intrinsic Role of Programmed Death-Ligand 1 in 2D and 3D Cell Culture Models of Human Breast Cancer

Katie Hudson[1], Neil Cross[1], Nicola Jordan-Mahy[1], Rebecca Leyland[1]

[1]Biomolecular Sciences Research Centre, City Campus, Sheffield Hallam University, Howard Street, Sheffield, S1 1WB

*corresponding author (R.Leyland@shu.ac.uk)

Introduction

- Tumorigenic expression of programmed death-ligand 1 (PD-L1) is found in many cancers and is well known to promote immune evasion and tumour progression through binding to its receptor PD-1 on T cells and other immune cells (Figure 1) (Jiang *et al.,* 2019).
- Monoclonal antibodies targeting PD-L1/PD-1 promote durable anti-tumour immune responses in select patients with advanced cancers, but most patients are unresponsive, hyperprogressive or develop resistance (Yang and Hu, 2019).
- The tumour-intrinsic role of PD-L1 and how immunotherapy treatment may influence its role remains poorly understood in all cancers.
- So far, most research investigating tumorigenic PD-L1 and its response to treatment is based on 2D cell culture models or immunocompromised mouse models that fail to recapitulate *in vivo* human tumours (Dong *et al.,* 2018; Hudson *et al.,* 2020).
- Better mimicking of the 3D architecture of solid tumours by utilising 3D cell culture models could provide an environment more representative of *in vivo* human tumours for the preclinical investigation of tumour-intrinsic PD-L1 signalling, response to immunotherapy treatment and cancer cell-immune cell interactions.

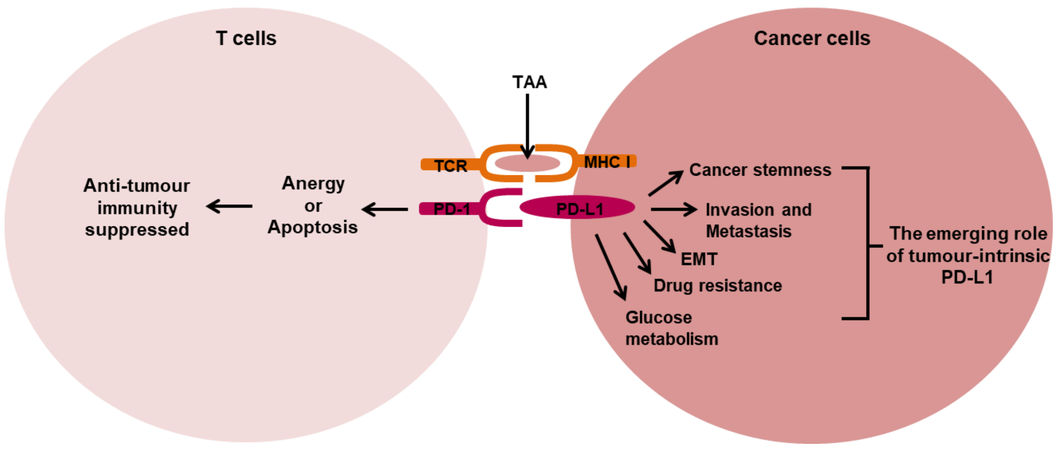

Figure 1. The new and emerging role of PD-L1 in some cancer cells. The role of PD-L1 to inhibit the immune system by binding to its receptor PD-1 expressed by T cells and other immune cells in the tumour microenvironment is well established, but recently PD-L1 has been shown to send pro-survivals in some cancer cells which may promote cancer initiation, epithelial to mesenchymal (EMT) transition, invasion and metastasis, drug resistance and metabolic activity. It is largely unknown whether anti-PD-L1 therapies can influence this new and emerging tumour-intrinsic role of PD-L1.

Research Aim

To determine the phenotypic effects of blocking PD-L1 with an anti-PD-L1 immunotherapy drug compared to knocking down PD-L1 in human breast cancer cells cultured in 2D and 3D cell culture models.

Methodology

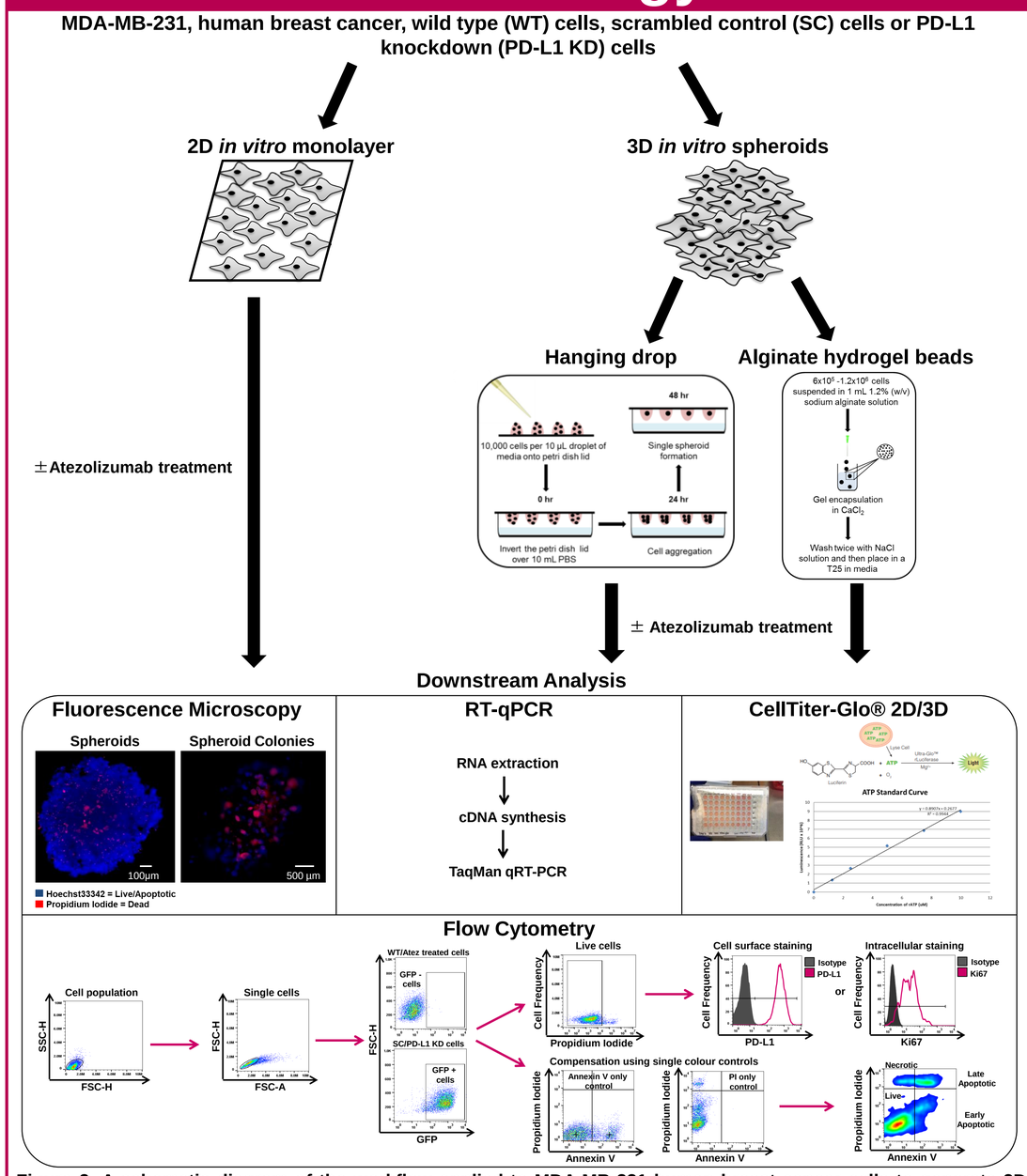

Figure 2. A schematic diagram of the workflow applied to MDA-MB-231 human breast cancer cells to generate 2D and 3D cell culture models for downstream analysis in order to determine the phenotypic effects of PD-L1 blockade compared to PD-L1 knockdown. MDA-MB-231 WT, SC and PD-L1 KD cells were cultured in 2D and 3D cell culture. The hanging drop method and alginate hydrogel beads were utilised to form 3D spheroids. Some cells in 2D and 3D culture were treated with anti-PD-L1 immunotherapy drug, Atezolizumab. 2D-cultured cells and 3D hanging drop spheroids were harvested at day 6 and 3D alginate spheroid colonies were harvested at 10 for downstream analysis. Cell viability was assessed using Hoechst/PI staining via fluorescent microscopy, CellTiter-Glo® via plate reader and Annexin V/PI staining via flow cytometry. PD-L1 mRNA and protein expression was measured via RT-qPCR and flow cytometry. Cell proliferation marker Ki67 was measured via intracellular flow cytometry staining. Appropriate controls and gating strategies were carried out for each experiment.

Results

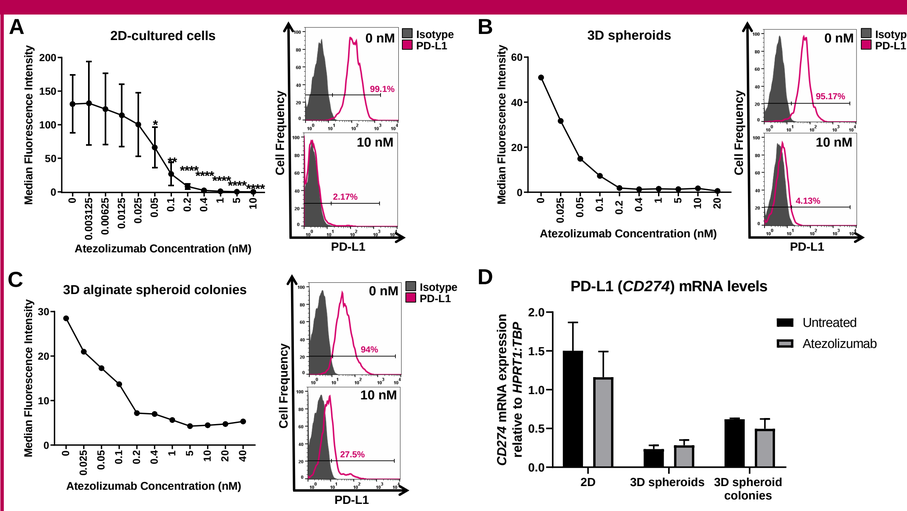

Figure 3. Atezolizumab blocks cell surface PD-L1 in a dose-dependent manner and does not effect the level of PD-L1 mRNA in 2D and 3D cultures. Flow cytometric analysis was used to determine the cell surface expression of PD-L1 on MDA-MB-231 breast cancer cells cultured in 2D and 3D following treatment with Atezolizumab at varying concentrations (0-40 nM). Representative flow cytometry plots are displayed for each culture system at concentrations of 0 nM and 10 nM demonstrating how Atezolizumab can completely block PD-L1 in 2D-cultured cells **(A)** and 3D spheroids **(B)**, but only partially block PD-L1 in 3D spheroid colonies. RT-qPCR was used to measure PD-L1 mRNA expression by 2D- and 3D-cultured cells following 10 nM Atezolizumab treatment. Atezolizumab treatment did not effect PD-L1 mRNA expression **(D)**. Data is presented as mean ± SD, n=3 independent experiments each with 3 technical repeats, Kruskal-Wallis followed by Conover Inman multiple comparison test, *P<0.05, **0.01, ****P<0.0001.

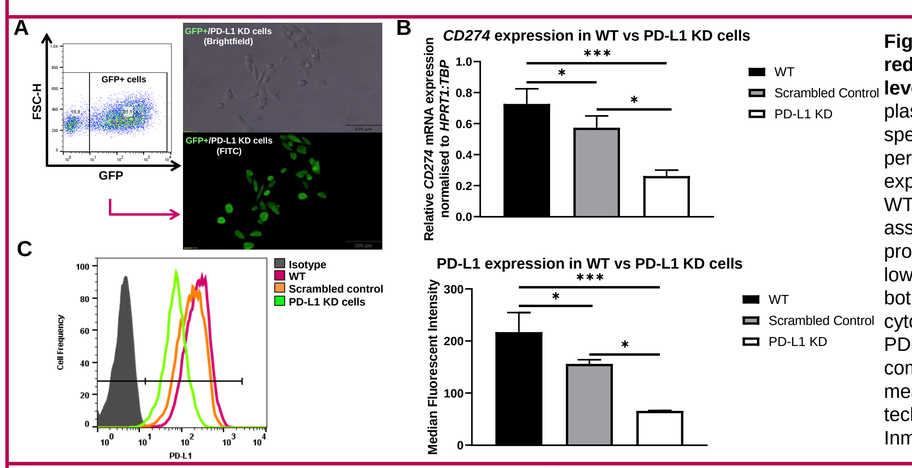

Figure 4. MDA-MB-231 PD-L1 KD cells display ~70% reduction in PD-L1 expression at mRNA and protein levels. MDA-MB-231 cells were stably transfected with a plasmid DNA encoding GFP upstream of our PD-L1-specific knockdown strategy. Clonal assays were performed to isolate a colony with homogenous expression of GFP and PD-L1 KD **(A)**. Scale bar 100 µM. WT, SC and PD-L1 KD cells were harvested and assessed for their expression of PD-L1 at mRNA **(B)** and protein **(C)** levels. PD-L1 KD cells express significantly lower levels of PD-L1 compared to WT and SC cells at both mRNA and protein levels. A representative flow cytometry plot is displayed to demonstrate the levels of PD-L1 protein expressed by WT, SC and PD-L1 KD cells compared to the isotype control. Data is presented as mean ± SD, n=3 independent experiments each with 3 technical repeats, Kruskal-Wallis followed by Conover Inman multiple comparison test, *P<0.05, ***0.001.

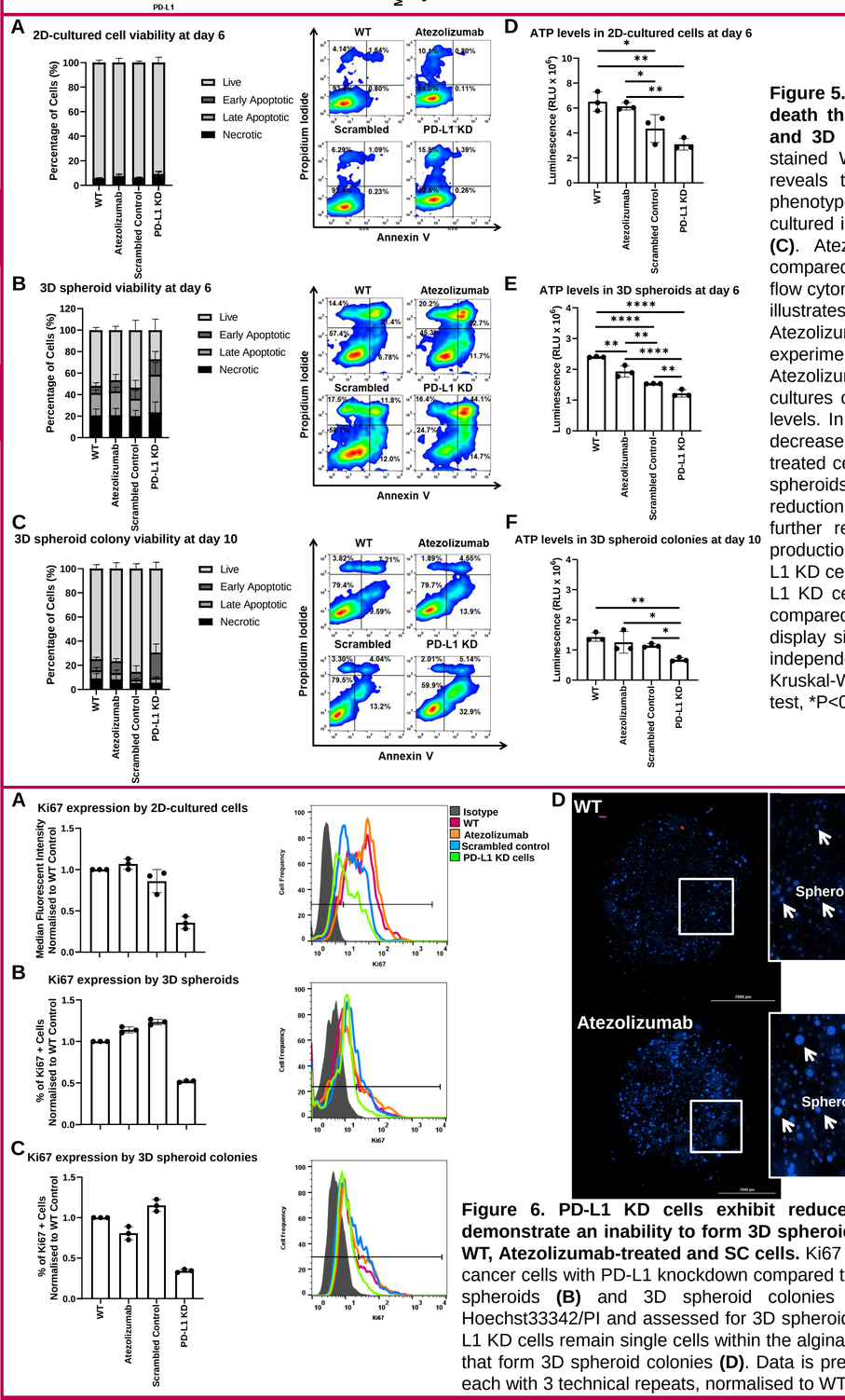

Figure 5. PD-L1 KD cells display a higher proportion of cell death than WT, Atezolizumab-treated and SC cells in 2D and 3D cultures. Flow cytometric analysis of Annexin V/PI stained WT, Atezolizumab-treated, SC and PD-L1 KD cells reveals that PD-L1 KD cells display an higher cell death phenotype compared to WT, Atezolizumab-treated and SC cells cultured in 2D **(A)**, 3D spheroids **(B)** and 3D spheroid colonies **(C)**. Atezolizumab induces slight changes in cell viability compared to WT cells in 2D and 3D cultures. Representative flow cytometry plots are displayed for 2D and 3D cultures which illustrates the differences in cell viability between WT, Atezolizumab-treated, SC and PD-L1 KD cells. CellTiter-Glo experiments were performed to validate the effects of Atezolizumab and PD-L1 KD on cancer cell death in 2D and 3D cultures compared to WT and/or SC cells via measuring ATP levels. In 2D cell culture, PD-L1 KD cells display a significant decrease in ATP levels compared to WT and Atezolizumab-treated cells but not SC cells, although still reduced **(D)**. In 3D spheroids, Atezolizumab-treated cells show a significant reduction in ATP levels compared to WT cells, which is even further reduced in PD-L1 KD cells **(E)**. The level of ATP production by cells in 3D spheroids is significantly lower in PD-L1 KD cells compared to SC cells. In 3D spheroid colonies, PD-L1 KD cells display a significant reduction in ATP production compared to WT, Atezolizumab-treated and SC cells which all display similar levels. Data is presented as mean ± SD, n=3 independent experiments each with 3 technical repeats, Kruskal-Wallis followed by Conover Inman multiple comparison test, *P<0.05, **P<0.01, ***0.001, ****P<0.0001.

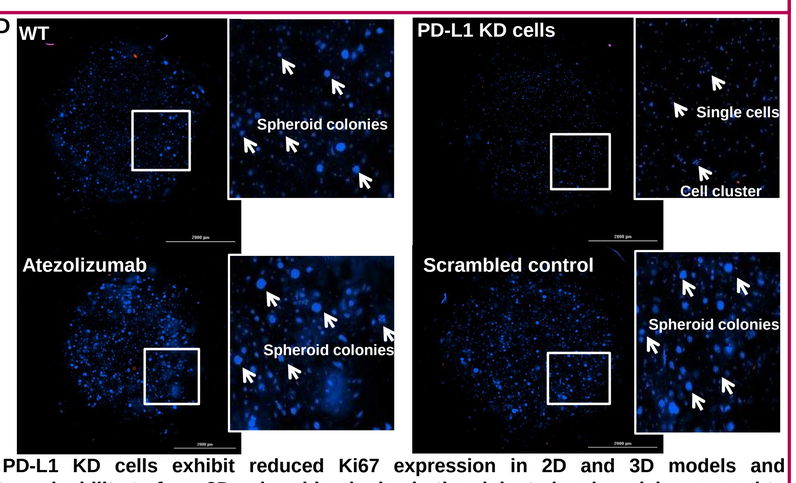

Figure 6. PD-L1 KD cells exhibit reduced Ki67 expression in 2D and 3D models and demonstrate an inability to form 3D spheroid colonies in the alginate bead model compared to WT, Atezolizumab-treated and SC cells. Ki67 staining reveals a lower proliferative capacity by breast cancer cells with PD-L1 knockdown compared to WT, Atezolizumab-treated and SC cells in 2D **(A)**, 3D spheroids **(B)** and 3D spheroid colonies **(C)**. Day 10 alginate beads were stained with Hoechst33342/PI and assessed for 3D spheroid colonies formation using fluorescent microscopy. PD-L1 KD cells remain single cells within the alginate compared to WT, Atezolizumab-treated and SC cells that form 3D spheroid colonies **(D)**. Data is presented as mean ± SD, n=3 independent experiments each with 3 technical repeats, normalised to WT cells either % or MFI. Scale bar represents 200 µM.

Conclusions

- Atezolizumab blocks cell surface PD-L1 but does not affect PD-L1 mRNA whereas PD-L1 knockdown reduces PD-L1 expression by ~70% at mRNA and protein levels
- PD-L1 knockdown cells show a higher proportion of cell death and reduced proliferative capacity in 2D and 3D models and are unable to form 3D spheroid colonies compared to WT and Atezolizumab-treated breast cancer cells
- By using 3D models that more closely mimic the characteristics of an *in vivo* human tumour, we show that targeting PD-L1 at the molecular level was able to disrupt the tumorigenic functions of PD-L1 more so than Atezolizumab

References

1. Jiang, X., Wang, J., Deng, X., Xiong, F., Ge, J., Xiang, B., Wu, X., MA, J., Zhou, M., Li, X., Li, Y., Li, G., Xiong, W., and Zeng, Z. (2019). Role of the tumor microenvironment in PD-L1/PD-1-mediated tumor immune escape. *Molecular Cancer*, 18 (1), 10. doi:10.1186/s12943-018-0928-4
2. Yang, J., and Hu, L. (2019). Immunomodulators targeting the PD-1/PD-L1 protein-protein interaction: From antibodies to small molecules. *Medicinal Research Reviews*, 39 (1): 265-301. doi:10.1002/med.21530
3. Dong, P., Xiong, Y., Yue, J., Hanley, S. J. B., and Watari, H. (2018). Tumor-intrinsic PD-L1 signalling in cancer initiation, development and treatment: Beyond immune evasion. *Frontiers in Oncology*, 8: 386. doi:10.3389/fonc.2018.00386
4. Hudson, K., Cross, N., Jordan-Mahy, N., and Leyland, R., (2020). The extrinsic and intrinsic roles of PD-L1 and its receptor PD-1: Implications for immunotherapy treatment. *Frontiers in Immunology*, 11: 568931. doi:10.3389/fimmu.2020.568931